Journal of Alzheimer's Disease 30 (2014) 91–100
DOI 10.3233/JAD-2012-111367
IOS Press

Towards a Dynamic Biomarker Model in Alzheimer's Disease

Abderazzak Mouiha[a] and Simon Duchesne[a,b,*], for the Alzheimer's Disease Neuroimaging Initiative[1]
[a]*Institut Universitaire en Santé Mentale de Québec, QC, Canada*
[b]*Radiology Department, Faculty of Medicine, Université Laval, QC, Canada*

Accepted 22 January 2012

Abstract. Biomarkers, both biological and imaging, are indicators of specific changes that characterize Alzheimer's disease (AD) progression *in vivo*. Knowing the precise relationship between biomarkers and disease severity would allow for accurate disease staging and possible forecasting of decline. Jack et al. suggested as an initial hypothesis that this relationship be sigmoidal; the objective of this article is to determine, using large-scale population data from ADNI, the precise shape of this association. We considered six different models (linear; quadratic; robust quadratic; local quadratic regression; penalized B-spline; and sigmoid) and used the Akaike Information Criterion to gauge how well these models compare in conforming to the data. We included 576 subjects (229 controls, 193 AD, and 154 mild cognitive impairment subjects who converted to AD) from the ADNI study, for whom baseline data on cerebrospinal fluid amyloid-β $(A\beta)_{42}$, phosphorylated tau (p-tau), and total-tau (t-tau), hippocampal volumes, and FDG-PET were available. Analysis of this cross-sectional dataset showed that a local quadratic regression model was 42% more likely than a sigmoid to be the best model for $A\beta_{42}$. This ratio augments to 22% and 73% for Penalized B-Spline in the case of p-tau and t-tau, respectively; to 3500% for the linear model for FDG-PET; and to 6700% for the Penalized B-Spline for hippocampal volumes. Preliminary, cross-sectional evidence therefore indicates that the shape of the association with disease severity is non-linear and differs between biomarkers.

Keywords: Akaike information criterion, Alzheimer's disease, biomarkers, dynamic model, statistical analysis

Supplementary data available online: http://dx.doi.org/10.3233/JAD-2012-111367

INTRODUCTION

Alzheimer's disease (AD) is a neuronal degeneration gradually altering cognitive abilities [1], leading to functional impairment and thus dementia. AD begins with abnormal processing of amyloid-β protein precursor, which results in excess production or reduced cleared of amyloid-β (Aβ) in the cortex [2]. By mechanisms as yet not completely known, this Aβ accumulation leads to a cascade characterized by abnormal tau aggregation, synaptic dysfunction, cell death, brain shrinkage, and cognitive deficits [3].

Biomarkers, both biological and imaging, are indicators of specific changes that characterize this progression *in vivo*. Evidence suggests that these AD biomarkers do not reach abnormal levels or peak simultaneously but do so in an ordered manner, consequent with disease progression. Petersen [4] and Jack et al. [5] have stated that disease progression is essentially biphasic, with biomarkers of Aβ deposition first to become abnormal (e.g., cerebrospinal fluid (CSF) Aβ), followed by neurodegeneration

[1]Data used in preparation of this article were obtained from the Alzheimer's Disease Neuroimaging Initiative (ADNI) database (http://adni.loni.ucla.edu). As such, the investigators within the ADNI contributed to the design and implementation of ADNI and/or provided data but did not participate in analysis or writing of this report. A complete listing of ADNI investigators can be found at: http://adni.loni.ucla.edu/wp-content/uploads/how_to_apply/ADNI_Acknowledgement_List.pdf

*Correspondence to: Simon Duchesne, Institut Universitaire en Santé Mentale de Québec, 2601 de la Canadiére, Room F-4435, G1J 2G3, QC, Canada. Tel.: (418) 663 5741; ext. 4777; Fax: (418) 663 5971; E-mail: simon.duchesne@crulrg.ulaval.ca.

biomarkers (e.g., CSF phosphorylated tau (p-tau) and total tau (t-tau); fluorodeoxyglucose uptake on positron emission tomography (FDG-PET); structural magnetic resonance imaging (MRI)).

In order for AD biomarkers to be used effectively for disease staging, their trajectories must be mathematically well characterized, and their time-dependent or "dynamic" ordering must be thoroughly understood [5]. Which model best represents this dynamism remains to be explained.

If the scope of observation is limited to the preclinical to clinical disease stages,[1] and hence regardless of an individual's starting point, there are three broad possibilities: either the rate of progression for biomarkers shows no variability, has a constant variability, or has a non-constant variability with time.

Linear models assume a constant progression (zero variability in rate of progression) over time; an example within the context of AD is FDG-PET hypometabolism [6]. Constant rates of progression can be approximated by power functions, either quadratic or higher-order, and represent an accelerating disease burden over time. There is some example evidence for a quadratic relationship in the reported global brain atrophy as individuals progress from MCI to typical, late-onset AD [7, 8]. Finally, non-constant rates of progression imply periods of acceleration and deceleration in the disease process. The simplest case is for one such complex, i.e., a sigmoid, as argued by Jack et al. Evidence to this effect can be found in mice studies [9]. The more involved case implies multiple phases of acceleration and deceleration; the deposition of Aβ oligomers has been shown to exhibit this type of relationship [10]. No strong evidence to date exists to our knowledge to imply that all biomarkers will follow a similar time course.

The objective of this article is to investigate the shape of this association between each biomarker and disease severity. The sigmoid hypothesis was originally tested by Caroli et al. [11], however, solely in comparison to linear regression. Without imposing *a priori* knowledge, we considered six different models of different orders in the present article.

These models (e.g., linear, sigmoid) are not nested, i.e., one is not a simplified version of another; hence, the statistical comparison approach taken in Caroli et al. is not entirely appropriate. Our chosen alternative is the Akaike Information Criterion (AIC), which can be used to compare two or more nested or non-nested models, based on different probability distributions. The AIC does not require the assumption that one of the candidate models is the "true" or "correct" model; as such, it is not a hypothesis test, does not have a *p*-value and does not use notions of significance. Rather, it focuses on the strength of evidence to gauge how well the models compete to conform to the data.

[1]Genetic, developmental, and lifelong environmental factors are likely contributors to an individual's biomarkers level status entering the preclinical to clinical phases of AD.

METHODS

Study population

In order to achieve scientific accuracy and statistical validity, the data needs to include numerous chemical and imaging biomarkers, collected longitudinally from large samples representing the full spectrum of the disease, including normal aging and its prodromal phase, referred to as mild cognitive impairment (MCI) [12]. To date, arguably the largest and best effort of this kind is the Alzheimer's Disease Neuroimaging Initiative (ADNI) [13].[2] To this end, in the first phase of the study, a total of 822 subjects were recruited at 58 sites throughout the United States and Canada for longitudinal follow-up.

As a convenient but admittedly crude first approximation, we elected to use cross-sectional baseline data from the ADNI study, as per the Caroli et al. article.

[2]*Data used in the preparation of this article were obtained from the Alzheimer's Disease Neuroimaging Initiative (ADNI) database (http://adni.loni.ucla.edu). The ADNI was launched in 2003 by the National Institute on Aging (NIA), the National Institute of Biomedical Imaging and Bioengineering (NIBIB), the Food and Drug Administration (FDA), private pharmaceutical companies, and non-profit organizations, as a $60 million, 5-year public-private partnership. The primary goal of ADNI has been to test whether serial magnetic resonance imaging (MRI), positron emission tomography (PET), other biological markers, and clinical and neuropsychological assessment can be combined to measure the progression of MCI and early AD. Determination of sensitive and specific markers of very early AD progression is intended to aid researchers and clinicians to develop new treatments and monitor their effectiveness, as well as lessen the time and cost of clinical trials. The Principal Investigator of this initiative is Michael W. Weiner, MD, VA Medical Center and University of California-San Francisco. ADNI is the result of efforts of many co-investigators from a broad range of academic institutions and private corporations, and subjects have been recruited from over 50 sites across the US and Canada. The initial goal of ADNI was to recruit 800 adults, ages 55 to 90, to participate in the research, approximately 200 cognitively normal older individuals to be followed for 3 years, 400 people with MCI to be followed for 3 years, and 200 people with early AD to be followed for 2 years. For up-to-date information, see http://www.adni-info.org.*

Thus, we included for this retrospective study all ADNI controls, AD, and MCI subjects who converted to AD on whom biomarker data were available.

All experiments were performed with the informed and overt consent of each participant or caregiver, in line with the Code of Ethics of the World Medical Association (Declaration of Helsinki) and the standards established by the Author's Institutional Review Board.

Biomarkers

Among the most studied biomarkers of AD, we select the following four in our experiments [11]:

- decreased CSF Aβ, as a marker of brain Aβ plaque deposition;
- increased CSF p-tau and t-tau, as an indicator of tau pathological changes and associated neuronal injury;
- decreased FDG-PET, used to measure net brain metabolism; and
- structural MRI measures of cerebral atrophy, especially hippocampal volumes, providing measures of cerebral atrophy caused by dendritic pruning and loss of synapses and neuron.

CSF acquisition was performed for a large subset of subjects and analyzed at the University of Pennsylvania ADNI Biomarker Core Laboratory. Post-processing included monoclonal antibodies specific for $A\beta_{42}$, t-tau, and p-tau phosphorylated at threonine 181. For modeling purposes, we used the $A\beta_{42}$, p-tau, and t-tau measurements only, as they were shown to correlate with clinical disease severity [14] and have been well validated and described in the course of the ADNI study [15].

FDG-PET scans were performed on a subset of subjects. All scans underwent quality control and pre-processing at the University of Michigan; post-processing analysis was performed at the University of Utah. For modeling purposes we used the average cerebral metabolic rate of glucose consumption in frontal, parietal, and temporal cortices, normalized to pons, as a measure of cerebral metabolism.

Volumetric MP-RAGE 1.5 Tesla MRI scans were collected for each subject. Following pre-processing at the University California, Los Angeles, left and right hippocampal volumes were semi-automatically computed at University of California, San Francisco, using a commercially available high dimensional brain mapping tool (Medtronic Surgical Navigation Technologies (SNT), Louisville, CO). For modeling purposes, we used the average of left and right hippocampal volumes.

The data used in this study was taken directly from the ADNI-controlled Study Data files (https://ida.loni.ucla.edu/login.jsp?project=ADNI%2f). Readers are referred to the ADNI procedure manuals (http://www.adni-info.org) for detailed descriptions of standardized data acquisition as well as biomarker pre- and post-processing.

Models description

We elected to test various linear and non-linear models for the association of biomarkers with disease severity. For each model a brief description follows, with prototypical curves shown in Fig. 1, and a complete mathematical description provided in Supplementary data (available online: http://www.j-alz.com/issues/30/vol30-1.html#supplementarydata02).

Linear models

A linear model (Fig. 1A) assumes that the relationship between the variables is constant; the starting point (intercept) may or may not be positive. Within the context of AD, net brain metabolism as measured via FDG-PET uptake has often been reported as a linear decline over time as the disease progresses [6].

Non-linear models

Variability in the rate of progression over time, i.e., acceleration or deceleration, implies a departure from linearity. Based on this criterion, we propose to examine two model classes.

Should this variability be constant, the model will follow a power law (e.g., x^2, x^3):

(i) We tested regular (see Fig. 1B) and robust versions of the quadratic model (see Fig. 1C), whereby the regression model parameters were estimated using a method less sensitive to outliers than the least squares estimates. Rates of whole brain atrophy in patients, as measured on MRI, have been shown to be accelerating as individuals progress from MCI to typical, late-onset AD [7, 8];

(ii) Locally fitting a model to the underlying data should increase overall fit. To this end, we used the locally weighted polynomial regression technique (LOESS), whereby at each point in the data set a low-degree polynomial was fitted to a subset of the data using weighted least

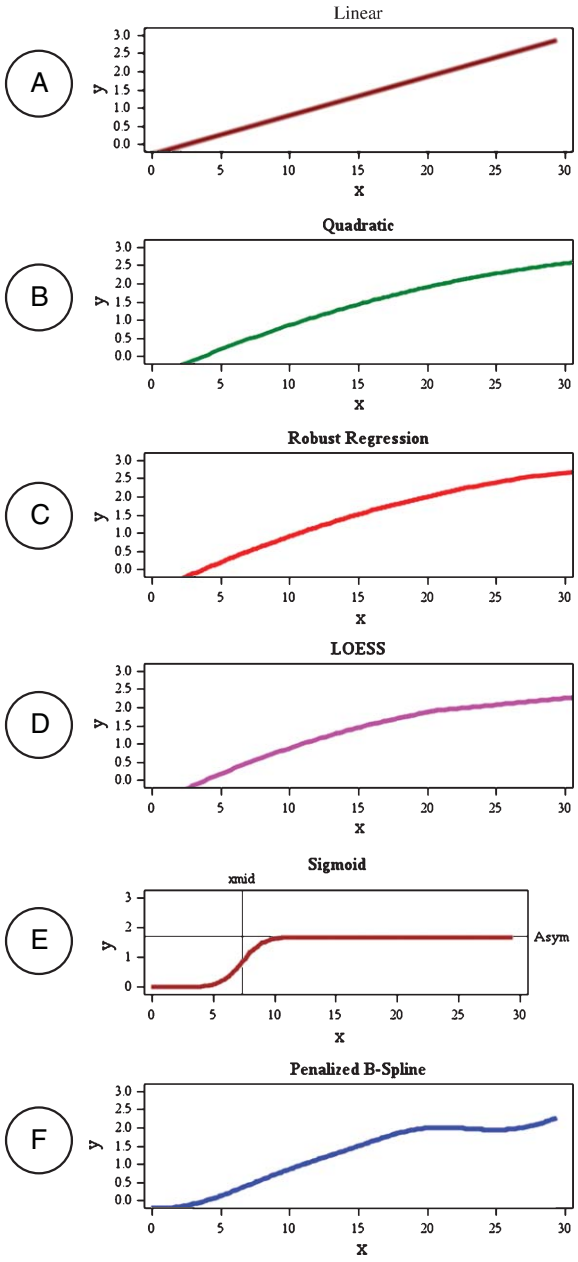

Fig. 1. Prototypical model curves.

squares, giving more weight to points near the point whose response is being estimated and less weight to points further away. Since we used a 2nd degree polynomial, in effect we employed a locally weighted quadratic model (see Fig. 1D). This has been used before to model the longitudinal course of ADAS-Cog scores [16].

Given that we used synthetic data to generate the prototypical curves of Fig. 1, the last three models are almost indiscernible to the naked eye.

Should the variability in the rate of progression not be constant, the model will be approximated by a spline – smoothly varying as a function of time.

(i) Within this model category we first examined the logistic function, commonly known as a sigmoid or S-curve (see Fig. 1E). This is a spline exhibiting only one inflection/deflection complex. It is characterized by an initial stage of growth, approximately exponential; then, as saturation begins, the growth slows, and at maturity, growth stops. As noted in Jack et al. [17], this implies that the maximum effect of each biomarker varies over the course of disease progression. Evidence to this effect can be found in mice studies [9];

(ii) A B-spline is a sufficiently smooth piecewise-polynomial function that can model multiple stages of growth and saturations, and even regressions (see Fig. 1F). The deposition of Aβ oligomers has been shown to exhibit this type of relationship [10].

Models comparison

All subjects were ordered based on their score on the AD assessment scale-cognitive (ADAS-Cog) as a surrogate marker of time. The ADNI dataset provides thus a "time-range" spanning the full spectrum of disease, from normal cognition through mild, moderate, and severe forms of AD. For the purpose of this study, we have chosen to limit our analysis on the range ADAS-Cog=[0, 30], given that there was a paucity of data at higher values (ADAS-Cog>30), which correspond to more advanced dementia state (see *Limitations*).

We plotted for each biomarker individual biomarker z-scores against ADAS-Cog, calculated sums of squares and R-squares in order to show model fit with the biomarkers data, and proceeded with fitting the six different models for each biomarker. The use of z-scores allows for easier comparison and interpretation of different biomarkers in subjects.

Given the number of models and difference in model order, we used the AIC for comparisons and model selection (see Supplementary data), a technique pioneered by Akaike [18] and used since in the medical literature as well (e.g., [19]). This criterion is optimized when the model has the maximum fit for the minimum number of parameters (simplicity and parsimony). By comparing AIC for different models, we can derive

Table 1
Study subject characteristics

	Controls ($n=229$)	MCI Converted AD ($n=154$)	Early AD ($n=95$)	Late AD ($n=98$)	p
Age (years)	76.0 ± 5.0	74.6 ± 7.0	75.3 ± 7.4	75.6 ± 7.6	0.21
Gender (female)	110 (48.03%)	60 (38.96%)	43 (45.26%)	48 (48.98%)	0.29
Education (years)	16.0 ± 2.9	15.7 ± 2.9	15.1 ± 2.9	14.3 ± 3.3	<0.0001
MMSE	29.1 ± 1.0	26.7 ± 1.7	25.2 ± 0.9	21.6 ± 1.2	<0.0001
ADAS-Cog	6.2 ± 2.9	13.3 ± 4.2	16.3 ± 5.5	20.9 ± 6.2	<0.0001
APOE ε4 (carriers)	61 (26.64%)	107 (69.48%)	65 (68.42%)	62 (63.27%)	<0.0001

Table 2
Biomarker characteristics

	Controls	MCI progressors	Early AD	Late AD	p
Total tau					
n	114	79	57	45	
pg/mL	69.7 ± 30.4	110.3 ± 51.1	113.9 ± 61.2	125.8 ± 57.6	<0.0001
Phosphorylated tau					
n	114	79	57	45	
pg/mL	24.9 ± 14.6	39.4 ± 15.8	38.7 ± 17.7	45.3 ± 21.8	<0.0001
$A\beta_{42}$					
n	114	79	57	45	
pg/mL	205.6 ± 55.1	141.9 ± 43.9	144.3 ± 45.8	141.3 ± 33.9	<0.0001
FDG-PET					
n	102	67	53	44	
CRMglc	1.4 ± 0.1	1.3 ± 0.1	1.3 ± 0.1	1.2 ± 0.1	<0.0001
Hippocampal volume					
n	159	119	63	66	
mL	2155 ± 297	1739 ± 363	1654 ± 356	1599 ± 323	<0.0001

a likelihood ratio describing how much support any model has over competing ones. We first report the likelihood ratios between linear and sigmoid models, and then all other models.

We performed statistical analyses using SAS 9.2 for windows (SAS/Stat, SAS/IML and SAS/Graph software, SAS, Cary, NC).

RESULTS

From the complete ADNI dataset, we included 576 subjects for whom baseline biomarker data were available: 229 healthy controls (age = 76 ± 5 years, 48% females), 154 MCI patients who converted to AD (age = 74 ± 7 years, 39% females, conversion time = 1.7 ± 0.8 years (6–36 months)), and 193 AD patients (age = 75 ± 7 years, 47% females). Summary sociodemographic, clinical, and neuropsychological statistical features for this population can be found in Table 1; biomarker information in Table 2.

Individual biomarker plots of z-scores against ADAS-Cog can be found in Fig. 2, and calculated SSq and R-squares of model fit with the biomarkers data can be found in Table 3. With higher R-square results, it would appear that $A\beta_{42}$ and hippocampus biomarkers had a better fit than t-tau and FDG-PET. Further, based solely on Table 3, it would appear as though the Penalized B-Spline model had a consistently better fit for all biomarkers. However, this model has more factors (covariates) than others and therefore, as discussed above, we calculated the AIC, Akaike weights, and evidence ratios to compare and select the best model for each biomarker. These are shown in Table 4.

The AIC evidence ratios measure how many times the best-fitting model is likely to be the best model in terms of AIC. The Sigmoid model was more likely than the Linear model to be the best fitting model by a factor of 5.5×10^5 for $A\beta_{42}$ (very strong likelihood); of 162.4 and 100.5 for p-tau and t-tau, respectively (strong likelihood); of -0.01 for FDG-PET (i.e., less likely); and 1.2 (i.e., just as likely) for hippocampus.

However, overall the Sigmoid, Quadratic, and Robust models were never as likely as other models. The most likely model for $A\beta_{42}$ was LOESS (AIC = -46.03; probability = 36.6% of being the best model); for p-tau, Penalized B-Spline (AIC = 259.33; probability = 83.4%), similarly for t-tau (AIC = 311.39; probability = 35.7%); for FDG-PET, Linear (AIC = -5.122; probability = 35.4%); and for hippocampus, Penalized B-Spline (AIC = 139.0; probability = 82.7%). These most likely models are shown, superimposed on the data, in Fig. 2.

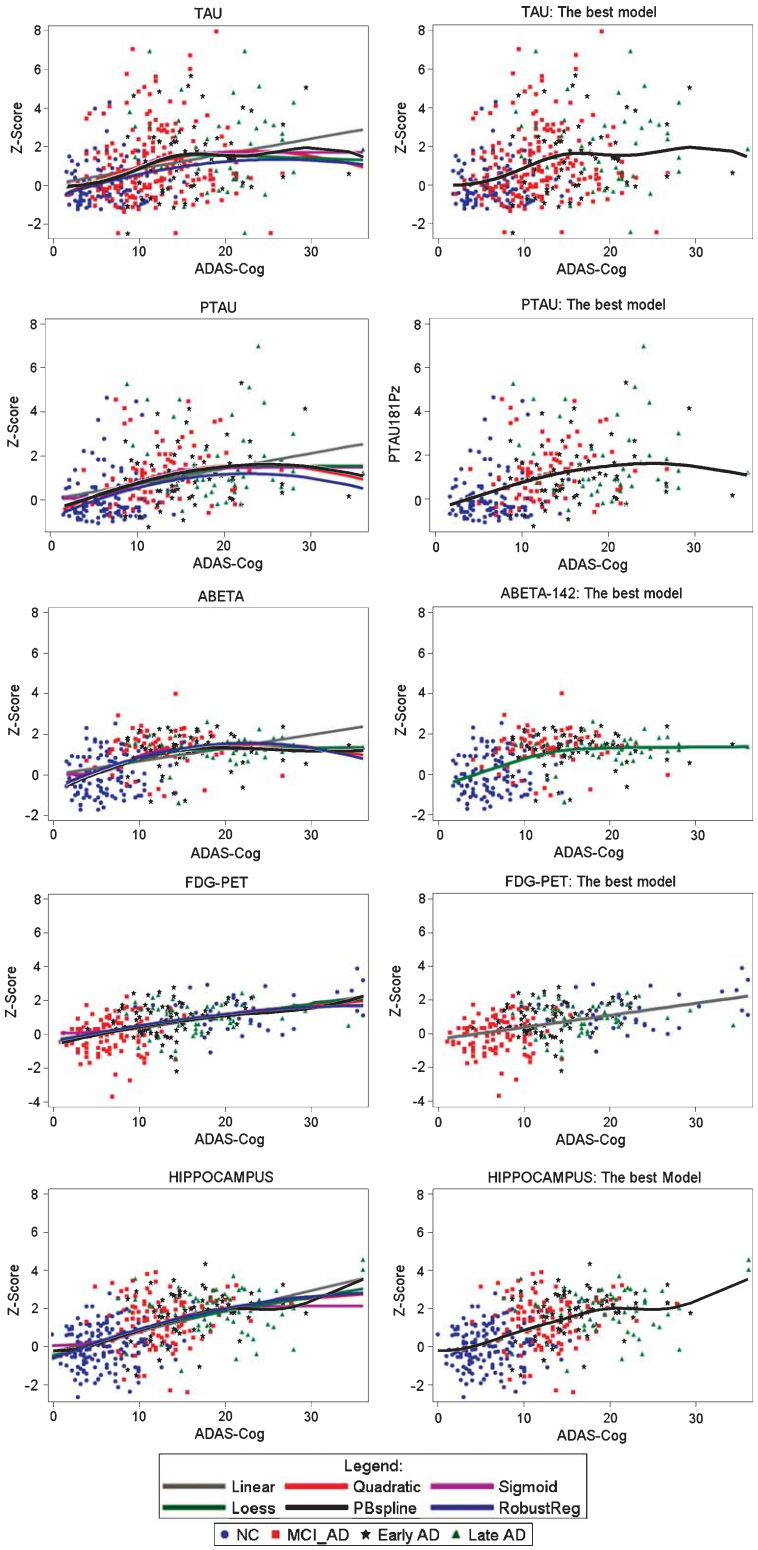

Fig. 2. Individual biomarker plots of z-scores against ADAS-Cog, with 6 models superimposed (left) and most likely model (right).

Table 3
Model fit estimates

Biomarker model	CSF p-tau		CSF t-tau		CSF $A\beta_{42}$		FDG-PET		Hippocampus	
	SSq	R^2	SSq	R^2	SSq	R^2	SSq	R^2	SSq	R^2
Linear	736.11	0.1830	860.33	0.0975	268.93	0.1816	255.11	0.2155	576.71	0.2715
Quadratic	703.64	0.2012	825.54	0.1340	248.87	0.2426	254.23	0.2182	569.01	0.2812
Robust	752.56	0.1721	854.47	0.1036	250.59	0.2374	256.06	0.2126	570.34	0.2795
PB-Spline	686.88	0.2279	819.45	0.1404	244.28	0.2566	252.76	0.2228	558.75	0.2942
LOESS	703.68	0.2010	831.80	0.1274	245.63	0.2525	254.42	0.2177	568.74	0.2815
Sigmoid	706.34	0.1997	828.09	0.1313	246.21	0.2507	260.05	0.2003	573.23	0.2759

SSq, sum of squares; R^2, R-square

Table 4
Akaike information criterion, weights, and evidence ratios

Model	Akaike information criterion/Akaike weights					Model/Evidence ratio				
	t-tau	*p*-tau	$A\beta_{42}$	FDG-PET	Hippo	t-tau	*p*-tau	$A\beta_{42}$	FDG-PET	Hippo
Linear	321.75	275.75	−21.30	−5.12	147.85	177.74	3671.19	235371.83	1.00	84.52
	0.002	0.000	0.000	0.354	0.010					
Quadratic	311.57	264.44	−42.17	−4.03	144.38	1.10	12.87	6.91	1.72	14.91
	0.326	0.065	0.053	0.206	0.056					
Robust	321.74	286.27	−40.14	−2.13	145.33	176.43	706536.21	19.08	4.46	24.03
	0.002	0.000	0.019	0.079	0.034					
PB-Spline	311.39	259.33	−45.66	−3.59	138.97	1.00	1.00	1.21	2.16	1.00
	0.357	0.834	0.303	0.164	0.827					
Local regression	313.80	264.46	−46.03	−3.84	144.19	3.34	12.99	1.00	1.90	13.58
	0.107	0.064	0.366	0.187	0.061					
Sigmoid	312.48	265.57	−45.33	1.98	147.39	1.73	22.60	1.42	34.89	67.13
	0.207	0.037	0.258	0.010	0.012					

For $A\beta_{42}$, the LOESS model is therefore 42% more likely to be the best model than the Sigmoid. For t-tau and p-tau, this ratio augments from 73% to 226% for Penalized B-Spline, respectively; for FDG-PET, 3500% for Linear, and 6700% for the Penalized B-Spline for hippocampus.

DISCUSSION

We proposed a thorough statistical analysis of baseline biomarker data within the timeline and context of the ADNI, and hence essentially in the preclinical to clinical phase of AD. The original hypothesis, as proposed in Jack et al. [6], was that the relationship between biomarkers and disease severity followed a sigmoid function.

Results show that within this timeframe, $A\beta_{42}$ had a piece-wise quadratic relationship with disease severity, as can be seen in Fig. 2A. The relationship displays immediate accumulation, which decreases with advanced disease state, and eventually plateaus. This pattern could be the tail-end of a sigmoid curve of accumulation as hypothesized by Jack and others, which seems to fit the data provided by PET studies with Aβ imaging compounds [20]. Alternatively, it suggests a non-zero intercept and hence a minimum level of amyloid deposition. Both of these explanations mean that early Aβ deposition has no discernable effect on cognition (ADAS-Cog remains null).

CSF measures of p-tau and t-tau as well as hippocampal volumes were best modeled using penalized B-splines, which corresponds to a quadratic fit between anchor points. As can be seen in Fig. 2B and D, both curves exhibit a repeating pattern of increase in severity, followed by a plateau. They appear to be temporally coupled with p-tau increases preceding t-tau (see Fig. 3). These data match previous evidence that rates of hippocampal atrophy and tau accumulation are not constant over time [21, 22]. The important aspect of a B-spline is its ability to have multiple inflexion points and thus multiple phases of accumulation/plateau; this is highly non-linear. Biologically, it would imply repeated attainment and disruptions of some form of homeostasis, for example with resumption of inflammatory [23] or neurovascular processes [24], as opposed to a continuous, uninterrupted neurodegeneration. Changes in tau may be related to different progression patterns in some forms of Aβ [9].

Finally, FDG-PET results indicate a linear decline with disease progression (Fig. 2C). This constant decrease in cerebral metabolism is indicative of decreased connectivity.

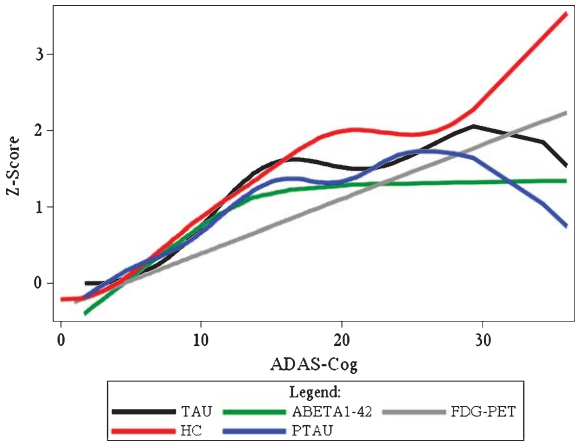

Fig. 3. Most likely models for each biomarker superimposed on similar disease severity scale show strong coupling of degeneration biomarkers for inter-subject cross-sectional data (105 subjects with all biomarkers at baseline).

Our FDG-PET results are also consistent with those obtained by Caroli et al. [11]; however, we find discrepant results for other biomarkers. This can be explained primarily from the fact that they did not test models other than linear and sigmoid; secondly, given the strongly non-linear nature of the data, it is not surprising to find that a sigmoidal model had the best fit. However, it does not mean it was the best non-linear model.

Limitations

These results may seem to disprove the sigmoidal hypothesis—that is, that each biomarker follows the same logistic curve, but should be interpreted in light of limitations.

For starters, models were not fit above ADAS-Cog>30 due to a paucity of data above that score; this precludes us from drawing conclusions on the behavior of the chosen biomarkers in late disease stages. This is a known limitation of the ADNI cohort in general, namely that probable AD subjects were not followed as long as other control or MCI subjects. We have attempted to mitigate this effect in our analysis by using robust techniques to remove the influence of outliers on model fit. In general, however, there is a risk using this data of painting a limited picture of the true full-course of AD, from pre-symptomatic to end of life. Model fitting in a short timeframe can be misleading; for example, a sigmoidal time course can appear to be linear or quadratic, depending on the time window; this might explain the FDG-PET results. Likewise, it would be unwise at this point to embark on observations regarding a lifelong AD process, given the limited timespan of the data we analyzed, as it would represent nothing more than mere conjectures. In order to expand the time course, one would have to possess a significantly large dataset of control, MCI, and AD subjects followed up for at least longer than a decade; such a dataset is cost prohibitive and few, if any, exist. It is likely that we will need to federate multiple databases together to arrive at a global picture of the time course of AD; inevitably, however, issues of standardization between studies must be resolved first before we can compare biomarker data.

A second issue is concerned with the use of the ADAS-Cog scale as a proxy of disease time course. The ADAS-Cog shows saturation effects at both ends of the cognition spectrum, common to other scales (e.g., Mini-Mental Status Examination (MMSE), Clinical Dementia Rating), notwithstanding their test-retest variability. To determine if ADAS-Cog was a major source of variability, we performed similar analyses using either another test (MMSE) or other biomarker (CSF t-tau) as proxies of disease time course (e.g., plot of hippocampal volume against CSF t-tau); the results were more or less identical (data not shown). In the end, we elected to maintain cognitive testing, and in particular ADAS-Cog, as the common denominator for biomarker model fit, given their critical importance in defining disease stages [25].

Secondly, and most obviously, the fit are based on a cross-sectional, single timepoint evaluation of multiple subjects. Further studies should be conducted using the rate of change in biomarkers with time to provide definite answers to the best disease trajectory. Preliminary evidence from Schuff et al. [26] on longitudinal data supports our baseline findings; yet, a sigmoidal relationship may still be the most apt representation of disease process, as 1-year results from Sabuncu et al. also propose [22]. Finally, we plotted the different biomarker curves with respect to disease severity in subjects for which all biomarkers were collected ($n_{Controls} = 39$; $n_{MCI\ convert} = 26$; $n_{Early\ AD} = 24$; $n_{Late\ AD} = 26$; total $n = 105$) (see Fig. 3). It can be appreciated that the time ordering is strongly coupled, rather than significantly temporally dissociated, as suggested in the theoretical model. This is strictly indicative, given that it compares baseline data, as mentioned previously.

Methodological considerations

We assessed six different models (linear; quadratic; LOESS; robust quadratic regression; sigmoid; and

penalized B-spline;) of different order and compared them using metrics based on the AIC. Due to its wider scope and statistical treatment, we evaluate that these results are more reliable than the previous analysis by Caroli et al.

It should be mentioned that results on higher power (e.g., x^3, x^4) and exponential functions, which would fall alongside quadratic fits within the first class of models, were inconclusive and therefore for the sake of clarity were not shown.

The AIC provides an objective way of determining which model among a set of specified models is the most parsimonious, based on a solid statistical principle (i.e., maximum likelihood). This is especially important when the specified models are not nested. In a loose sense, we can say that Model A is nested within Model B if Model A is a special case of Model B; this is not our case as we try to compare various model families. We agree, however, that this criterion is only as good as the data underlying the fit, and the conclusions will depend on the set of candidate models specified. Therefore, it can be said that the AIC model selection technique only selects the best model from the specified set; it does not detect if a better model exists.

In our opinion, the sample size is large enough for each model fit, and thus the penalty term (second term in eq. 8) provides an adequate bias adjustment. Because of the large effective sample size, the use of a second-order AIC*c* is unnecessary, because AIC*c* and AIC converge as *n/p* gets large [27]. This is showed by this equation:

$$AIC_c = n.\ln(SS_q/n) + 2p + \frac{2p(p+1)}{n-p-1} \text{converges to } AIC \text{ as } n \text{ gets larger.}$$

It remains that to have an unbiased AIC, the true model must be in the family of candidate models. If this assumption is violated, the AIC criterion can be biased.

CONCLUSION

Initial analysis of cross-sectional multi-centric ADNI baseline data empirically support a linear progression in FDG-PET hypometabolism, and non-linear progression for CSF Aβ, p-tau, and t-tau accumulation as well as hippocampal atrophy throughout the various phases of AD.

ACKNOWLEDGMENTS

This work was supported by funding from the Ministère du Développement Économique, de l'Innovation et de l'Exportation du Québec; the Fonds de recherche en santé du Québec; and the National Science and Engineering Research Council of Canada.

We thank Drs A. Caroli and G.B. Frisoni from the Laboratory for Epidemiology, Neuroimaging and Telemedicine, IRCCS Fatebenefratelli San Giovanni Di Dio, Brescia, Italy, for their help in the preparation of the data and comments on the manuscript.

Data collection and sharing for this project was funded by the Alzheimer's Disease Neuroimaging Initiative (ADNI) (National Institutes of Health Grant U01 AG024904). ADNI is funded by the National Institute on Aging, the National Institute of Biomedical Imaging and Bioengineering, and through generous contributions from the following: Abbott; Alzheimer's Association; Alzheimer's Drug Discovery Foundation; Amorfix Life Sciences Ltd.; AstraZeneca; Bayer HealthCare; BioClinica, Inc.; Biogen Idec Inc.; Bristol-Myers Squibb Company; Eisai Inc.; Elan Pharmaceuticals Inc.; Eli Lilly and Company; F. Hoffmann-La Roche Ltd and its affiliated company Genentech, Inc.; GE Healthcare; Innogenetics, N.V.; Janssen Alzheimer Immunotherapy Research & Development, LLC.; Johnson & Johnson Pharmaceutical Research & Development LLC.; Medpace, Inc.; Merck & Co., Inc.; Meso Scale Diagnostics, LLC.; Novartis Pharmaceuticals Corporation; Pfizer Inc.; Servier; Synarc Inc.; and Takeda Pharmaceutical Company. The Canadian Institutes of Health Research is providing funds to support ADNI clinical sites in Canada. Private sector contributions are facilitated by the Foundation for the National Institutes of Health (http://www.fnih.org). The grantee organization is the Northern California Institute for Research and Education, and the study is coordinated by the Alzheimer's Disease Cooperative Study at the University of California, San Diego. ADNI data are disseminated by the Laboratory for Neuro Imaging at the University of California, Los Angeles. This research was also supported by NIH grants P30 AG010129, K01 AG030514, and the Dana Foundation.

Authors' disclosures available online (http://www.j-alz.com/disclosures/view.php?id=1148).

REFERENCES

[1] McKhann G, Drachman D, Folstein M, Katzman R, Price D, Stadlan EM (1984) Clinical diagnosis of Alzheimer's

disease: Report of the NINCDS-ADRDA Work Group under the auspices of Department of Health and Human Services Task Force on Alzheimer's Disease. *Neurology* **34**, 939-944.

[2] Blennow K, de Leon MJ, Zetterberg H (2006) Alzheimer's disease. *Lancet* **368**, 387-403.

[3] Oddo S, Caccamo A, Tran L, Lambert MP, Glabe CG, Klein WL, LaFerla FM (2006) Temporal profile of amyloid-beta (Abeta) oligomerization in an *in vivo* model of Alzheimer disease. A link between Abeta and tau pathology. *J Biol Chem* **281**, 1599-1604.

[4] Petersen RC (2010) Alzheimer's disease: Progress in prediction. *Lancet Neurol* **9**, 4-5.

[5] Jack CR Jr, Knopman DS, Jagust WJ, Shaw LM, Aisen PS, Weiner MW, Petersen RC, Trojanowski JQ (2010) Hypothetical model of dynamic biomarkers of the Alzheimer's pathological cascade. *Lancet Neurol* **9**, 119-128.

[6] Mosconi L, Mistur R, Switalski R, Tsui WH, Glodzik L, Li Y, Pirraglia E, De Santi S, Reisberg B, Wisniewski T, de Leon MJ (2009) FDG-PET changes in brain glucose metabolism from normal cognition to pathologically verified Alzheimer's disease. *Eur J Nucl Med Mol Imaging* **36**, 811-822.

[7] Chan D, Janssen J, Whitwell J, Watt H, Jenkins R, Frost C, Rossor M, Fox N (2003) Change in rates of cerebral atrophy over time in early-onset Alzheimer's disease: Longitudinal MRI study. *Lancet* **362**, 1121-1122.

[8] Knight WD, Kim LG, Douiri A, Frost C, Rossor MN, Fox NC (201) Acceleration of cortical thinning in familial Alzheimer's disease. *Neurobiol Aging* **32**, 1765-1773.

[9] Garcia-Alloza M, Robbins EM, Zhang-Nunes SX, Purcell SM, Betensky RA, Raju S, Prada C, Greenberg SM, Bacskai BJ, Frosch MP (2006) Characterization of amyloid deposition in the APPswe/PS1dE9 mouse model of Alzheimer disease. *Neurobiol Dis* **24**, 516-524.

[10] Oddo S, Caccamo A, Tran L, Lambert MP, Glabe CG, Klein WL, LaFerla FM (2006) Temporal profile of amyloid-beta (Abeta) oligomerization in an *in vivo* model of Alzheimer disease. A link between Abeta and tau pathology. *J Biol Chem* **281**, 1599-1604.

[11] Caroli A, Frisoni GB (2010) The dynamics of Alzheimer's disease biomarkers in the Alzheimer's Disease Neuroimaging Initiative cohort. *Neurobiol Aging* **31**, 1263-1274.

[12] Petersen RC (2004) Mild cognitive impairment as a diagnostic entity. *J Intern Med* **256**, 183-194.

[13] Mueller SG, Weiner MW, Thal LJ, Petersen RC, Jack CR, Jagust W, Trojanowski JQ, Toga AW, Beckett L (2005) Ways toward an early diagnosis in Alzheimer's disease: The Alzheimer's Disease Neuroimaging Initiative (ADNI). *Alzheimers Dement* **1**, 55-66.

[14] Blennow K, Vanmechelen E, Hampel H (2001) CSF total tau, Abeta42 and phosphorylated tau protein as biomarkers for Alzheimer's disease. *Mol Neurobiol* **24**, 87-97.

[15] Shaw LM, Vanderstichele H, Knapik-Czajka M, Clark CM, Aisen PS, Petersen RC, Blennow K, Soares H, Simon A, Lewczuk P, Dean R, Siemers E, Potter W, Lee VM, Trojanowski JQ (2009) Cerebrospinal fluid biomarker signature in Alzheimer's disease neuroimaging initiative subjects. *Ann Neurol* **65**, 403-413.

[16] Ito K, Corrigan B, Zhao Q, French J, Miller R, Soares H, Katz E, Nicholas T, Billing B, Anziano R, Fullerton T (2011) Disease progression model for cognitive deterioration from Alzheimer's Disease Neuroimaging Initiative database. *Alzheimers Dement* **7**, 151-160.

[17] Jack CR Jr, Knopman DS, Jagust WJ, Shaw LM, Aisen PS, Weiner MW, Petersen RC, Trojanowski JQ (2010) Hypothetical model of dynamic biomarkers of the Alzheimer's pathological cascade. *Lancet Neurol* **9**, 119-128.

[18] Akaike H (1983) Information measures and model selection. *Int Stat Inst* **44**, 277-291.

[19] Sormani M, Stromillo ML, Battaglini M, Signori A, De Stefano N (2011) Modelling the distribution of cortical lesions in multiple sclerosis. *Mult Scler* **18**, 229-231.

[20] Rowe CC, Ellis KA, Rimajova M, Bourgeat P, Pike KE, Jones G, Fripp J, Tochon-Danguy H, Morandeau L, O'Keefe G, Price R, Raniga P, Robins P, Acosta O, Lenzo N, Szoeke C, Salvado O, Head R, Martins R, Masters CL, Ames D, Villemagne VL (2010) Amyloid imaging results from the Australian Imaging, Biomarkers and Lifestyle (AIBL) study of aging. *Neurobiol Aging* **31**, 1275-1283.

[21] Mouiha A, Duchesne S (2011) Hippocampal atrophy rates in Alzheimer's disease: Automated segmentation variability analysis. *Neurosci Lett* **495**, 6-10.

[22] Sabuncu MR, Desikan RS, Sepulcre J, Yeo BT, Liu H, Schmansky NJ, Reuter M, Weiner MW, Buckner RL, Sperling RA, Fischl B (2011) The Dynamics of cortical and hippocampal atrophy in Alzheimer disease. *Arch Neurol* **68**, 1040-1048.

[23] Parachikova A, Agadjanyan MG, Cribbs DH, Blurton-Jones M, Perreau V, Rogers J, Beach TG, Cotman CW (2007) Inflammatory changes parallel the early stages of Alzheimer disease. *Neurobiol Aging* **28**, 1821-1833.

[24] Iadecola C (2004) Neurovascular regulation in the normal brain and in Alzheimer's disease. *Nat Rev Neurosci* **5**, 347-360.

[25] McKhann GM, Knopman DS, Chertkow H, Hyman BT, Jack CR Jr, Kawas CH, Klunk WE, Koroshetz WJ, Manly JJ, Mayeux R, Mohs RC, Morris JC, Rossor MN, Scheltens P, Carillo MC, Thies B, Weintraub S, Phelps CH (2011) The diagnosis of dementia due to Alzheimer's disease: Recommendations from the National Institute on Aging and the Alzheimer's Association workgroup. *Alzheimers Dement* **7**, 263-269.

[26] Schuff N, Insel P, Chiang G, Truran D, Gamst A, Jack C, Aisen P, Petersen R, Shaw L, Trojanowski J, Weiner M (2011) Acceleration of brain atrophy rates with advancing cognitive deterioration from normal aging to MCI to Alzheimer's disease. *Alzheimers Dement* **7**, S223-S223.

[27] Burnham KP, Anderson DR (2001) Kullback-Leibler information as a basis for strong inference in ecological studies. *Wildlife Res* **28**, 111-119.